

## Oscillator strength and electron-impact excitation of the Schumann-Runge continuum of the oxygen molecule

Sunggi Chung and Chun C. Lin

Department of Physics, University of Wisconsin, Madison, Wisconsin 53706

(Received 6 August 1979)

By using the method of multiconfiguration self-consistent field, the electronic wave functions for the  $X^3\Sigma_g^-$  and  $B^3\Sigma_u^-$  states of  $O_2$  are determined for twelve values of internuclear distances. From the appropriate electronic-vibrational functions, the oscillator strengths for the  $X^3\Sigma_g^- \rightarrow B^3\Sigma_u^-$  absorption (Schumann-Runge) continuum are calculated over the energy range of 7–9.5 eV. The results are in good agreement with experiments except at the high-energy edge (above 9 eV) which corresponds to the very steeply varying part of the potential curve. A calculation of the electron-impact excitation cross sections for the  $B^3\Sigma_u^-$  state with the Born-Ochkur approximation is also reported for incident electron energy up to 1000 eV.

### I. INTRODUCTION

The Schumann-Runge system of  $O_2$  has received a great deal of attention in molecular spectroscopy.<sup>1</sup> The role it plays in producing metastable oxygen atoms ( $^1D$ ) in the upper atmosphere is of much importance in aeronomy.<sup>2</sup> The potential curve for the upper state ( $B^3\Sigma_u^-$ ) has a shallow minimum at an internuclear distance considerably larger than the equilibrium distance of the  $X^3\Sigma_g^-$  ground state. As a result the  $X^3\Sigma_g^- \rightarrow B^3\Sigma_u^-$  absorption is composed of mainly a continuum over a few eV (with a set of very weak bands at the low-frequency end), i.e., the Schumann-Runge continuum. The oscillator strengths of the Schumann-Runge continuum over the absorption energy range of 7–10 eV have been measured in several laboratories.<sup>3–6</sup> The problem of theoretical calculation of these oscillator strengths is important from the standpoint of electronic structure of the  $O_2$  molecule. Because of the open-shell structure of the lowest electronic configuration, the ground electronic state (also the lower excited states) exhibits strong configuration interaction. This renders the use of single-configuration self-consistent-field (SCF) wave functions inadequate. Calculations of the  $X^3\Sigma_g^- \rightarrow B^3\Sigma_u^-$  transition moment for several internuclear distances have been reported<sup>7,8</sup>; indeed the effect of configuration mixing was found to be quite important. While the theoretical values of the transition moment appear to be in general accord with experiment, a direct comparison cannot be made since the transition moment itself was not measured directly, but only inferred from the observed absorption intensity.

In this paper we present a calculation of the oscillator strength of the  $X^3\Sigma_g^- \rightarrow B^3\Sigma_u^-$  continuum as a function of the absorption energy and com-

pare our results with those determined experimentally. Good agreement is found except for those transitions terminating at the very steeply ascending part of the  $B^3\Sigma_u^-$  potential curve. Included in our work is also a study of electron-impact excitation to the  $B^3\Sigma_u^-$  state.

### II. OSCILLATOR STRENGTH

The dominant configuration of the  $X^3\Sigma_g^-$  ground state of  $O_2$  is

$$(1\sigma_g)^2(1\sigma_u)^2(2\sigma_g)^2(2\sigma_u)^2(3\sigma_g)^2(1\pi_u)^4(1\pi_g)^2,$$

and that of  $B^3\Sigma_u^-$  is

$$(1\sigma_g)^2(1\sigma_u)^2(2\sigma_g)^2(2\sigma_u)^2(3\sigma_g)^2(1\pi_u)^3(1\pi_g)^3.$$

A single-configuration wave function  $\psi$  is an antisymmetrized product of one-electron molecular-orbital (MO) functions  $\phi_i(\vec{r}_i, R)$  with  $\vec{r}_i$  denoting the  $i$ th electron coordinates and  $R$  the internuclear separation. Each MO is in turn expanded by a finite set of basis functions  $\eta_1, \eta_2, \dots$  as

$$\phi_i = \sum_p \eta_p c_{ip} = \eta c_i. \quad (1)$$

Under this single-configuration approximation, the SCF method leads to a well-known pseudo-eigenvalue equation,<sup>9</sup>

$$F_i c_i = \sum_j S_{ij} c_j \epsilon_{ji}, \quad (2)$$

which is the prescription for determining the orbital coefficients  $c$ . The Fock matrix  $F$  depends on these coefficients, and thus Eq. (2) has to be solved iteratively. The overlap matrix  $S$  arises as no orthogonality condition is imposed on the basis functions  $\eta$ . The orbital functions  $\phi$  are constrained to be orthonormal by means of

the Lagrangian multipliers  $\epsilon_{jj}$ .

A considerable improvement is realized by expressing the wave function  $\Psi$  as linear combinations of single-configuration functions  $\psi_j$ ; i.e.,

$$\Psi(\vec{r}_1, \vec{r}_2, \dots, R) = \sum_j a_j(R) \psi_j(\vec{r}_1, \vec{r}_2, \dots, R), \quad (3)$$

where  $a(R)$  are called configuration coefficients. One way to determine these coefficients is to diagonalize the matrix associated with

$$\sum_k (H_{jk} - \delta_{jk} E_j) a_k = 0, \quad (4)$$

where

$$H_{jk} = \int \psi_j^* H \psi_k d\tau, \quad (5)$$

and  $H$  is the appropriate Hamiltonian for the molecule. This is the essence of the method of configuration interaction (CI). As no provision is made for improving the orbital-expansion coefficients  $c$  in the multiconfiguration environment, a large number of configurations are needed in the CI method. An alternative to CI is to extend the SCF procedure to the multiconfiguration form of Eq. (3). This was proposed by Hinze and Root-haan,<sup>10</sup> and further expanded by Huzinaga.<sup>11</sup> In the method of multiconfiguration self-consistent field (MCSCF), we start with a wave function of the form Eq. (3) determined by the CI procedure, and allow the orbital coefficients  $c$  to vary with the set of configuration coefficients fixed. Analogous to Eq. (2), the new values of  $c$  are determined from the equation

$$\sum_j A_{ij} c_j = \sum_k S c_k \epsilon_{ik}. \quad (6)$$

Here the Fock matrices due to various configurations are coupled via the configuration coefficients to form the  $A$  matrix. It is noted, however, that the orbital coefficients  $c$  are common to all constituent single-configuration functions  $\psi$  in Eq. (3). Following the suggestion of Ref. 11, we solve Eq. (6) linearly for the first-order correction term  $\delta c$ . In other words, with the known values of  $c$  from the  $n$ th iterative stage, we substitute

$$c^{(n+1)} = c^{(n)} + \delta c \quad (7)$$

in Eq. (6) and solve for  $\delta c$  by retaining only the first-order terms. Using the improved values of  $c$ , we recalculate the configuration coefficients  $a$ , and the cycle is repeated. All steps of the MCSCF procedure are meticulously detailed in Refs. 10 and 11. A general iterative procedure leading to self-consistency may be summarized as follows:

(i) Solve a single (dominant) configuration SCF to obtain starting  $c$ .

(ii) With  $c$  as given, determine the coefficients  $a$  by Eq. (4).

(iii) Construct  $A_{ij}$  from the coefficients  $a$  of step (ii) and solve for  $\delta c$ .

(iv) Repeat steps (ii) and (iii) until a desired self-consistency ( $|\delta c| < 10^{-5}$ ) is achieved.

In this work we used a basis set consisting of five  $s$ -type contracted Gaussian-type orbitals (GTO) constructed from ten individual GTO, and four  $p$ -type contracted GTO from six individual Gaussians. The exponents of the Gaussians as well as the contraction coefficients are given in Ref. 12. In order to keep the computational work within a manageable scope, we take the  $1\sigma_g$  and  $1\sigma_u$  orbitals as being always doubly occupied and consider only those configurations resulting from all possible assignments of the remaining 12 electrons to the  $2\sigma_g$ ,  $2\sigma_u$ ,  $3\sigma_g$ ,  $1\pi_u$ ,  $1\pi_g$ ,  $3\sigma_u$  orbitals. This leads to 30 configurations consistent with  ${}^3\Sigma_g^-$  symmetry, and 28 configurations with  ${}^3\Sigma_u^-$ . In Tables I and II we present these configurations along with the mixing coefficients and the total energy for the  $X^3\Sigma_g^-$  and  $B^3\Sigma_u^-$  states, respectively, at the equilibrium internuclear distance for the ground state (1.2 Å).

In the cases where more than two MO are partially filled, two or more distinct Slater determinants are derived from a given set of occupational numbers due to different spin assignments. For example, we take a linear combination of the two Slater determinants associated with the configuration labeled as 9 in Table I; i.e.,

$$(1/\sqrt{2}) [ | \dots (1\pi_u^+ \alpha)(1\pi_u^- \beta)(1\pi_g^+ \alpha)(1\pi_g^- \alpha) | - | \dots (1\pi_u^+ \beta)(1\pi_u^- \alpha)(1\pi_g^+ \alpha)(1\pi_g^- \alpha) | ],$$

in order to conform to the  $X^3\Sigma_g^-$  symmetry (with  $M_S = 1$ ). Likewise the appropriate combination for configuration 10 in Table I is

$$(1/\sqrt{2}) [ | \dots (1\pi_u^+ \alpha)(1\pi_u^- \alpha)(1\pi_g^+ \alpha)(1\pi_g^- \beta) | - | \dots (1\pi_u^+ \alpha)(1\pi_u^- \alpha)(1\pi_g^+ \beta)(1\pi_g^- \alpha) | ].$$

Further details may be found in Ref. 13.

Denoting the MC electronic wave functions for the  $X^3\Sigma_g^-$  and  $B^3\Sigma_u^-$  states as  $\Psi_X$  and  $\Psi_B$ , respectively, we compute the transition-moment matrix element as

$$z_{XB}(R) = \int \Psi_B^*(\vec{r}_1, \vec{r}_2, \dots, R) \times \left( \sum_{k=1}^{16} z_k \right) \Psi_X(\vec{r}_1, \vec{r}_2, \dots, R) d\vec{r}_1 \cdots d\vec{r}_{16}, \quad (8)$$

TABLE I. Configurations<sup>a</sup> for the  $X^3\Sigma_g^-$  state at  $R=1.2 \text{ \AA}$ .

									Coefficients	
	$2\sigma_g$	$2\sigma_u$	$3\sigma_g$	$3\sigma_u$	$1\pi_u^+$	$1\pi_u^-$	$1\pi_g^+$	$1\pi_g^-$	30-conf. SCF	5-conf. SCF
1	2	2	2	0	2	2	1	1	0.956 082	0.960 931
2	2	2	0	2	2	2	1	1	-0.072 058	-0.064 694
3	2	2	2	0	1	1	2	2	-0.199 331	-0.188 520
4	2	2	0	2	1	1	2	2	0.039 208	
5	0	2	2	2	2	2	1	1	-0.029 427	
6	2	0	2	2	2	2	1	1	-0.014 419	
7	2	1	2	1	2	2	1	1	0.122 624	0.128 960
8	2	1	2	1	2	2	1	1	-0.037 672	
9	2	2	2	2	1	1	1	1	0.021 566	
10	2	2	2	2	1	1	1	1	-0.000 094	
11	1	2	1	2	2	2	1	1	-0.041 254	
12	1	2	1	2	2	2	1	1	0.000 191	
13	2	2	1	1	1	2	2	1	-0.127 933	-0.142 297
14	2	2	1	1	1	2	2	1	0.008 548	
15	2	2	1	1	1	2	2	1	-0.009 622	
16	1	2	2	1	1	2	2	1	0.055 217	
17	1	2	2	1	1	2	2	1	-0.008 658	
18	1	2	2	1	1	2	2	1	0.002 904	
19	0	2	2	2	1	1	2	2	0.008 228	
20	2	0	2	2	1	1	2	2	0.003 764	
21	1	2	1	2	1	1	2	2	0.022 654	
22	1	2	1	2	1	1	2	2	-0.000 504	
23	2	1	2	1	1	1	2	2	-0.031 174	
24	2	1	2	1	1	1	2	2	0.006 808	
25	2	1	1	2	1	2	2	1	0.025 786	
26	2	1	1	2	1	2	2	1	-0.000 533	
27	2	1	1	2	1	2	2	1	0.005 620	
28	1	1	2	2	1	2	2	1	0.002 310	
29	1	1	2	2	1	2	2	1	0.001 286	
30	1	1	2	2	1	2	2	1	-0.002 463	
Total energy (in a.u.)									-149.708	-149.496

<sup>a</sup>Configurations are specified by the occupation numbers of MO.

where the summation covers all 16 electrons of the  $O_2$  molecule. To study the Schumann-Runge system, let us consider a transition from the lowest vibrational level of the  $X^3\Sigma_g^-$  state ( $X0$ ) to a continuum vibrational level of the  $B^3\Sigma_u^-$  state which is labeled by the index  $W$  corresponding to the energy of this vibrational level as measured from the dissociation limit of the  $B^3\Sigma_u^-$  state. The continuum vibrational wave functions  $\chi_W(B|R)$  are determined from the potential curve of the  $B^3\Sigma_u^-$  state<sup>14</sup> by using the procedure outlined in the Appendix of Ref. 15. The oscillator strength for this  $X0 \rightarrow BW$  transition is

$$f(X0 \rightarrow BW) = (2\Delta E/3) \left| \int \chi_W^*(B|R) z_{XB}(R) \times \chi_0(X|R) R^2 dR \right|^2, \quad (9)$$

where  $\chi_0(X|R)$  is the wave function of the ground vibrational level of  $X^3\Sigma_g^-$ , and  $\Delta E$  is the excitation energy. If we normalize  $\chi_W$  so that the density of states over an energy range of 1 eV is unity, then

$f(X0 \rightarrow BW)$  is equivalent to the quantity  $df/dE$  given in Fig. 4 of Ref. 6.

At  $R=1.2 \text{ \AA}$  (equilibrium internuclear distance of the ground state), we obtain the transition moment  $z_{XB}$  as 0.873 a.u. which may be compared with 0.920 a.u. reported by Julienne, Neumann, and Krauss.<sup>8</sup> This agreement is quite remarkable in view of the fact that the manifold of configurations selected for their MCSCF calculation as well as their basis set for constructing molecular orbitals are different from ours. To illustrate the importance of configuration mixing, we decompose the transition moment into contributions from various configuration pairs by combining Eqs. (3) and (8); i.e.,

$$z_{XB}(R) = \sum_{ij} a_i^X(R) a_j^B(R) \times \int \psi_j^*(\vec{r}_1, \vec{r}_2, \dots, R) \times \left( \sum_{k=1}^{16} z_k \right) \psi_i(\vec{r}_1, \vec{r}_2, \dots, R) d\vec{r}_1 \cdots d\vec{r}_{16}. \quad (10)$$

TABLE II. Configurations<sup>a</sup> for the  $B^3\Sigma_u^-$  states at  $R=1.2 \text{ \AA}$ .

									Coefficients	
	$2\sigma_g$	$2\sigma_u$	$3\sigma_g$	$3\sigma_u$	$1\pi_u^+$	$1\pi_u^-$	$1\pi_g^+$	$1\pi_g^-$	28-conf. SCF	5-conf. SCF
1	2	2	2	0	2	1	1	2	0.903 183	0.912 644
2	2	2	0	2	2	1	1	2	-0.012 380	
3	2	0	2	2	2	1	1	2	-0.027 354	
4	2	1	2	1	2	1	1	2	0.079 494	0.117 096
5	2	1	2	1	2	1	1	2	-0.000 534	
6	2	1	2	1	2	1	1	2	-0.036 249	
7	0	2	2	2	2	1	1	2	-0.021 400	
8	2	2	1	1	2	2	1	1	0.374 944	0.365 003
9	2	2	1	1	2	2	1	1	0.049 311	
10	2	2	1	1	1	1	2	2	0.109 441	0.117 028
11	2	2	1	1	1	1	2	2	0.003 832	
12	1	2	2	1	2	2	1	1	-0.077 988	0.080 289
13	1	2	2	1	2	2	1	1	-0.025 139	
14	1	2	2	1	1	1	2	2	-0.066 132	
15	1	2	2	1	1	1	2	2	-0.000 042	
16	2	1	1	2	2	2	1	1	-0.079 394	
17	2	1	1	2	2	2	1	1	-0.015 914	
18	2	1	1	2	1	1	2	2	-0.015 732	
19	2	1	1	2	1	1	2	2	-0.004 150	
20	2	2	2	2	2	1	0	1	-0.042 689	
21	2	2	2	2	0	1	2	1	0.022 660	
22	1	2	1	2	2	1	1	2	-0.003 645	
23	1	2	1	2	2	1	1	2	-0.000 996	
24	1	2	1	2	2	1	1	2	0.001 298	
25	1	1	2	2	1	1	2	2	-0.004 650	
26	1	1	2	2	1	1	2	2	0.002 139	
27	1	1	2	2	2	2	1	1	-0.013 389	
28	1	1	2	2	2	2	1	1	0.004 883	
Total energy (in a.u.)									-149.333	-149.184

<sup>a</sup>Configurations are specified by the occupation numbers of MO.

The integrals in Eq. (10) may be one of the five types shown in Table III. In Table IV we list the contributions from each pair of configurations at  $R=1.2 \text{ \AA}$ . One notices that only a few configurations are important as far as the  $X \rightarrow B$  absorption intensity is concerned. From a series of test calculations, we find little change in the transition-moment matrix element if we limit the number of configurations to five (configurations 1, 2, 3, 7, 13) for the ground state and to five (1, 4, 8, 10, 12) for the upper state. This allows us to greatly reduce the numerical work. The configuration coefficients and total energy derived from this five-configuration MCSCF calculation for the  $X^3\Sigma_g^-$  and  $B^3\Sigma_u^-$  states are included in the last column of Tables I and II, respectively. The dipole matrix elements computed from these five-configuration wave functions are given in Table III and are quite close to the results of the full calculation involving 30 configurations for  $X^3\Sigma_g^-$  and 28 for  $B^3\Sigma_u^-$ . A breakdown of the contribution from the various configuration pairs to the transition moment for the five-configuration calculation

is shown in Table IV. The transition moment varies from 0.891 to 0.873 a.u. between the five-configuration and the full calculation. But if configuration mixing is entirely neglected, the value of the transition moment becomes almost twice as large. This clearly indicates the inadequacy of the single-configuration approximation for the case of  $O_2$ . Using the five-configuration scheme, we calculate the transition moment at twelve values of  $R$  from 0.9 to 2.0  $\text{\AA}$  and, with the aid of the appropriate vibrational wave functions, the

TABLE III. Dipole matrix elements at  $R=1.2 \text{ \AA}$ .

Configurations	$(30 \times 28)^a$	$(5 \times 5)^b$	
1	$\langle 1\pi_u   z   1\pi_g \rangle$	1.182 825	1.148 174
2	$\langle 3\sigma_g   z   3\sigma_u \rangle$	-1.117 884	-1.106 711
3	$\langle 3\sigma_g   z   2\sigma_u \rangle$	-1.253 562	-1.244 049
4	$\langle 2\sigma_g   z   3\sigma_u \rangle$	0.141 830	0.149 521
5	$\langle 2\sigma_g   z   2\sigma_u \rangle$	-0.887 668	-0.892 271

<sup>a</sup>30 configurations for the  $X^3\Sigma_g^-$  state and 28 for  $B^3\Sigma_u^-$ .

<sup>b</sup>5 configurations for the  $X^3\Sigma_g^-$  state and 5 for  $B^3\Sigma_u^-$ .

oscillator strength  $f(X0 \rightarrow BW)$  for the continuum in the excitation range of 7–9.5 eV which is shown in Fig. 1 along with the experimental data of Ref. 6. (Earlier measurements reported by other workers<sup>3-5</sup> agree well with those of Ref. 6 and are not shown here.) We see very good agreement between theory and experiment at energies up to 9 eV. For absorption above this energy, we are dealing with the steeply ascending part of the potential curve which is subject to a higher degree of uncertainty than the lower part. This reduces the accuracy of the continuum vibrational wave function and therefore the oscillator strength. It is likely that the low-frequency side of the observed continuum spectrum contains, in addition to the  $X \rightarrow B$  absorption, transition from the ground state to a  ${}^3\Pi_u$  state which is of repulsive

TABLE IV. Contributions to transition moment.

Configurations		Type <sup>a</sup>	Contribution	
X	B		(30 × 28) <sup>b</sup>	(5 × 5) <sup>c</sup>
1	1	1	1.444 464	1.424 022
1	8	2	-0.566 726	-0.548 957
3	1	1	-0.301 152	-0.279 372
13	1	2	0.182 671	0.203 258
13	8	1	-0.080 239	-0.084 337
7	8	3	0.057 635	0.058 559
2	8	2	0.042 713	0.036 959
3	10	2	0.034 488	0.034 530
13	10	1	0.023 421	0.027 041
7	4	1	0.016 306	0.024 520
1	12	4	-0.014 956	-0.016 314
13	4	3	0.012 749	0.020 728
7	16	2	0.010 883	
2	16	3	0.010 142	
16	1	4	-0.010 003	
7	12	5	-0.008 489	-0.009 239
16	12	1	0.007 203	
4	10	2	-0.006 784	
16	14	1	0.006 108	
16	4	5	-0.003 896	
11	12	2	0.003 597	
11	16	5	-0.002 907	
3	14	4	0.002 644	
13	2	2	0.002 504	
8	9	3	-0.002 329	
8	6	1	0.002 284	
11	8	4	0.002 194	
6	16	3	0.002 031	
2	2	1	0.001 492	
4	18	3	0.001 094	
9	20	1	0.001 089	
5	7	1	0.001 053	
others			0.001 998	
total			0.873 282	0.891 398

<sup>a</sup>Types are as listed in Table III.

<sup>b</sup>30 configurations for the  $X^3\Sigma_g^-$  state and 28 for  $B^3\Sigma_u^-$ .

<sup>c</sup>5 configurations for the  $X^3\Sigma_g^-$  state and 5 for  $B^3\Sigma_u^-$ .

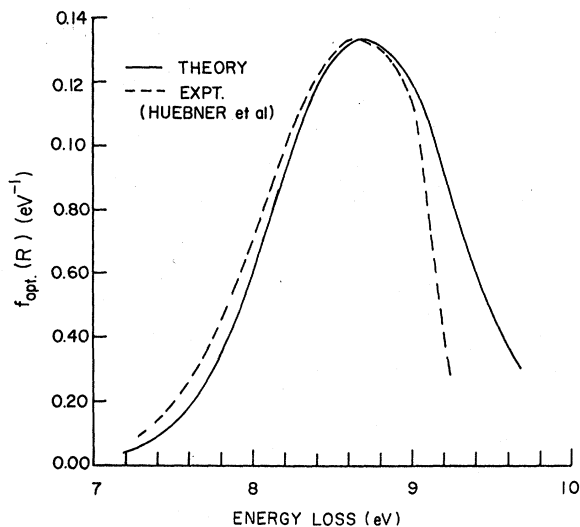


FIG. 1. Optical oscillator strengths of the Schumann-Runge continuum. The solid curve is the present theory, and the dashed one represents the experimental data of Ref. 6.

nature lying somewhat below  $B^3\Sigma_u^-$ . Wilkinson and Mulliken<sup>16</sup> suggested that the total oscillator strength of  $X \rightarrow {}^3\Pi_u$  is on the order of 0.01. This may account for the experimental oscillator strengths at 7–8.5 eV (as shown in Fig. 1) being somewhat larger than the theoretical values which do not include the  $X \rightarrow {}^3\Pi_u$  contribution.

### III. DISSOCIATIVE EXCITATION OF THE $B^3\Sigma_u^-$ STATE BY ELECTRON IMPACT

Closely related to the photoabsorption process discussed in Sec. II is the electron-impact excitation of the  $B^3\Sigma_u^-$  state. Since the  $B^3\Sigma_u^-$  state is an optically allowed one, the electron-impact

TABLE V. Electron-impact excitation (dissociation) cross sections of the  $B^3\Sigma_u^-$  state in  $10^{-17}$  cm<sup>2</sup>.

eV	Cross section
10	3.13
15	6.57
20	7.29
25	7.21
30	6.91
40	6.20
50	5.56
75	4.40
100	3.64
150	2.74
200	2.21
300	1.62
500	1.08
1000	0.93

excitation cross sections may be expected to be fairly large. Moreover, excitation of  $B^3\Sigma_u^-$  furnishes a mechanism for generating metastable  $O(^1D)$  atoms which is of considerable interest in atmospheric physics.<sup>2</sup> For cross-section calculations, we use the Born approximation to treat direct excitation and the Ochkur modification for exchange excitation. For this  $X0 \rightarrow BW$  excitation produced by electron impact, the incident and scattered electron are associated, respectively, with the  $X0$  and the  $BW$  target states; thus the initial and final electron wave vectors are written as  $\vec{k}_{X0}$  and  $\vec{k}_{BW}$ , respectively. We denote their difference by

$$\vec{K} \equiv \vec{k}_{X0} - \vec{k}_{BW}, \quad (11)$$

and the relative orientation between  $\vec{K}$  and the molecular axis by the polar and azimuthal angles  $\Theta$  and  $\Phi$ . The transition amplitude is

$$\begin{aligned} \epsilon_{XB}(K, R, \Theta, \Phi) = & - \int \Psi_B^*(\vec{r}_1, \vec{r}_2, \dots, \vec{R}) \left( \sum_{i=1}^{16} e^{i\vec{K} \cdot \vec{r}_i} \right) \\ & \times \Psi_X(\vec{r}_1, \vec{r}_2, \dots, \vec{R}) d\vec{r}_1 \dots d\vec{r}_{16}. \end{aligned} \quad (12)$$

The differential cross sections in the  $(\theta, \phi)$  direction for the  $X0 \rightarrow BW$  excitation are

$$I_{BW}(\theta, \phi) = (k_{BW}/4\pi k_{X0}) \int \sin\Theta d\Theta d\Phi \left| \int \chi_{BW}^*(R) \chi_{X0}(R) (2K^{-2} - k_{X0}^{-2}) \epsilon_{XB}(K, R, \Theta, \Phi) R^2 dR \right|^2. \quad (13)$$

Application of the Born approximation to electron-impact excitation of electronic states of diatomic molecules has been discussed in our earlier work.<sup>15,17</sup> [Eq. (13) here differs slightly from Eq. (8) of Ref. 15 which contains a typographical error.<sup>18</sup>] Integration of  $I_{BW}$  over  $\theta$  and  $\phi$  gives the cross sections for excitation to a unit energy range about  $W$  of the repulsive state, viz.,

$$Q(X0 \rightarrow BW) = \int I_{BW}(\theta, \phi) \sin\theta d\theta d\phi. \quad (14)$$

It follows that the cross sections of excitation to the entire repulsive part of the  $B^3\Sigma_u^-$  state are

$$Q(X \rightarrow B) = \int Q(X0 \rightarrow BW) dW. \quad (15)$$

Details about the computational procedure can be found in Refs. 15 and 17. Since the excitation to the bound levels of  $B^3\Sigma_u^-$  (i.e.,  $X0 \rightarrow Bv$ ) are very weak in comparison with the continuum part, Eq. (15) gives essentially the excitation cross section to the entire  $B^3\Sigma_u^-$  electronic states.

With the same set of wave functions that were used for calculating oscillator strengths, we obtain the cross sections  $Q(X \rightarrow B)$  from Eq. (15) for incident electron energies up to 1000 eV, and the results are summarized in Table V. Although no attempt was made to locate the exact position of

the peak, the cross section  $7.29 \times 10^{-17}$  cm<sup>2</sup> at 20 eV should be quite close to the maximum value. Since the two states ( $X \rightarrow B$ ) are connected by a dipole transition, the excitation function is expected to be broad, decreasing only as  $\ln E/E$  at large incident-electron energies.<sup>19</sup> We find that the present cross sections conform to such asymptotic form around 300 eV within  $\sim 10\%$ . By extrapolating the measured differential cross-section data, Trajmar *et al.*<sup>20</sup> report a cross section of  $8.6 \times 10^{-17}$  cm<sup>2</sup> at 20 eV which is in reasonable agreement with our calculation, but their cross section ( $11.5 \times 10^{-17}$  cm<sup>2</sup>) at 45 eV is much larger than the present result. Since the Born-approximation cross sections become more accurate at higher energies, one would not expect a larger discrepancy at 45 eV. Additional experimental work on cross-section measurement is needed.

#### ACKNOWLEDGMENT

The work reported in this paper was supported by the DNA (Atmospheric Effect Division) under Subtask No. S99QAX-H 1004-W.U.97 LABCEDE Program. The authors wish to thank Dr. Edward T. P. Lee for calling their attention to the importance of the metastable oxygen atoms in atmospheric physics.

<sup>1</sup>P. H. Krupenie, *J. Phys. Chem. Ref. Data* **1**, 423 (1972).

<sup>2</sup>See, for example, R. C. Schaffer and P. D. Feldman, *J. Geophys. Res.* **77**, 6828 (1972); M. H. Rees and D. Luckey, *ibid.* **79**, 5181 (1974); M. H. Rees, J. C. G. Walker, and A. Dalgarno, *Planet. Space Sci.* **15**, 1097 (1967).

<sup>3</sup>K. Watanabe, E. C. Y. Inn, and M. Zelickoff, *J. Chem. Phys.* **21**, 1026 (1953).

<sup>4</sup>P. H. Metzger and G. R. Cook, *J. Quant. Spectrosc. Radiat. Transfer* **4**, 107 (1964).

<sup>5</sup>R. Goldstein and F. N. Mastrup, *J. Opt. Soc. Am.* **56**, 765 (1966).

<sup>6</sup>R. H. Huebner, R. J. Celotta, S. R. Mielczarek, and

- C. E. Kuyatt, *J. Chem. Phys.* 63, 241 (1975).
- <sup>7</sup>B. J. Moss and W. A. Goddard, *J. Chem. Phys.* 63, 3523 (1975).
- <sup>8</sup>P. S. Julienne, D. Neumann, and M. Krauss, *J. Chem. Phys.* 64, 2990 (1976).
- <sup>9</sup>C. C. J. Roothaan, *Rev. Mod. Phys.* 23, 69 (1951); 32, 179 (1960).
- <sup>10</sup>J. Hinze and C. C. J. Roothaan, *Prog. Theor. Phys. Suppl.* 40, 37 (1967).
- <sup>11</sup>S. Huzinaga, *Prog. Theor. Phys.* 41, 307 (1969).
- <sup>12</sup>T. H. Dunning, Jr., *J. Chem. Phys.* 55, 716 (1971).
- <sup>13</sup>M. Kotani, Y. Mizuno, K. Kayama, and E. Ishiguro, *J. Phys. Soc. Jpn.* 12, 707 (1957).
- <sup>14</sup>P. H. Krupenie, *J. Phys. Chem. Ref. Data* 1, 423 (1972), Table 53.
- <sup>15</sup>S. Chung, C. C. Lin, and E. T. P. Lee, *Phys. Rev. A* 12, 1340 (1975).
- <sup>16</sup>P. G. Wilkinson and R. S. Mulliken, *Astrophys. J.* 125, 594 (1957).
- <sup>17</sup>S. Chung and C. C. Lin, *Phys. Rev. A* 6, 988 (1972).
- <sup>18</sup>The integral in Eq. (8) of Ref. 15 should read  $\int |\int \chi_{nw}^*(R) \chi_{00}(R) (2K^{-2} - T^{-2}) \epsilon_{0n}(K, R, \Theta, \Phi) R^2 dR|^2 \times \sin \Theta d\Theta d\Phi$ , and similarly for Eq. (9) of Ref. 15.
- <sup>19</sup>N. F. Mott and H. S. W. Massey, *The Theory of Atomic Collisions*, 3rd ed. (Oxford, Univ. Press, New York, 1965), Chap. XVI.
- <sup>20</sup>S. Trajmar, W. Williams, and A. Kuppermann, *J. Chem. Phys.* 56, 3759 (1972).